CDF MUON DETECTION

Lee G. Pondrom

University of Wisconsin-Madison

ABSTRACT

The muon detection system now being constructed for CDF is briefly described. This system is composed of magnetized iron toroids covering the polar angle range $3^o < \theta < 17^o$ with respect to both circulating p's and $\bar{p}$'s, and a central muon detector covering $\pm 35^o$ about 90^o to the beams. Muons above about 3 GeV/c $p_\perp$ are identified at the trigger level by requiring tracks to be straight within the spatial resolution of the trigger hardware and to penetrate 6 λ_a or more of Fe. At the trigger level the rate is dominated by $\pi \to \mu$ decays in flight. An initial trigger rate at 10^{30} cm^{-2} sec^{-1} luminosity of 100 hz for single muons can be decreased to a few hz by using more complete fast pattern recognition. Proposed enhancement of the muon coverage as a part of the detector upgrade is also described.

INTRODUCTION

Efficient muon detection in $\bar{p}$-p collider experiments is important for several reasons. Prompt muons are a signature of weak decays of heavy quark flavors and weak intermediate bosons. Heavy flavor cascade decay can lead to several muons, or a combination of muons and electrons. For example, in the decay $t \to b \to c \to s$ a pair of leptons might be observed, with the same charge or opposite charges depending on where they occurred in the sequence. Neutrinos accompany weak leptonic decays, and their detection is possible only through their missing transverse energy, which requires measurement of all of the visible energy of an event. Since muons represent an important component of the visible energy, their identification and energy measurement are crucial for good neutrino detection.

Muons are the most penetrating of the charged elementary particles, so that muon detectors are usually placed furthest from the interaction region, on the outside of the central detector. Six or more absorption lengths of material typically shield the muon chambers or counters from the colliding beams. This absorber may be instrumented for electromagnetic and hadronic calorimetry. A magnetic field region, either in Fe absorber or in a low density tracking volume before the calorimeters, measures the muon momentum.

There are two types of background to muon detection. A pion or kaon can decay in flight into a muon, giving a real muon which is not derived from an interesting source. Or a hadron, usually a pion, can "punch-through" the iron absorber, faking a muon in appearance. In this case the particle which punches through is often in fact a muon created by $\pi \to \mu$ decay in the hadronic cascade in the absorber, but need not be. Both types of background fall off sharply with increasing transverse momentum, so good muon detectors tend to employ thick absorbers and $p_{\perp}$ thresholds above 1 GeV/c.

Since muon counters are placed outside of the detector behind thick shielding, the valid muon trigger rate is low, even at high luminosity. This feature makes the muon system an important part of any detector trigger scheme.

CDF MUON DETECTORS

A. SCOPE OF COVERAGE

Table 1 shows the geometrical parameters of the CDF muon system.[1] An elevation view of the hardware is shown in Fig. 1. The small angle system, composed of magnetized Fe toroids on the axis of the colliding beams, covers polar angles $3^\circ < \theta < 17^\circ$, identifies muons by penetration through 3 m of Fe, and employs 15° sectored drift chambers with wires along chords of concentric circles to measure the momentum. An end view of an instrumented toroid is shown in Fig. 2. The central system covers $55^\circ < \theta < 125^\circ$, uses the central electromagnetic and hadronic calorimeters as shielding, and 1.5 T central solenoidal magnetic field for deflection. Muons are detected by a ring of drift tubes surrounding the calorimeter modules with drift wires parallel to the colliding beam axis. The forward system acceptance is $\Delta\eta = 3.6$, while the central acceptance is $\Delta\eta = 1.3$. The gap between 17° and 55° is 2 units (both ends), and 11 units of rapidity at 2 TeV are lost in the beam pipes at angles less than 3°.

B. BASIC DETECTOR ELEMENTS

Figure 3 shows an end view of the solenoid field, one 15° calorimeter wedge module, and the associated muon drift tubes. An extrapolated impact parameter b at the center of the solenoid is defined by the muon trajectory in the drift tubes. Equal drift times means a radial muon track. The times are compared in the trigger with a 30 nsec resolution, which corresponds to an uncertainty in impact parameter $\Delta b = 10$ cm, or $p_\perp = 5$ GeV/c. The multiple scattering in the calorimeter is comparable to this uncertainty. This 5 GeV/c uncertainty in the impact parameter means that many low momentum tracks satisfy the trigger. The actual momentum measurement is made in the solenoid field, however, where the error is much smaller $\Delta p_\perp/p_\perp = 0.0008\, p_\perp$ (GeV/c).

Figure 4 shows the toroid bend plane and the configuration of drift chamber wires. The trigger cells in the drift chambers form towers which point to the interaction volume. The widths of the trigger cells grow with radius, which gives both a constant bite in pseudo-rapidity and a constant $p_\perp$ threshold. The basic trigger is again a straight track through the drift chambers, called 1 * 3 * 3, where a front cell is OR'd with three cells in each of the other two planes. Muon momentum is measured from the sagitta of the drift times in the three chambers, with the incident angle as an extra constraint. The multiple scattering is a fixed fraction of the deflection in the magnetic field independent of momentum:

$$\theta_{MS}/\theta_{BEND} = 0.18.$$

The trigger efficiencies as a function of $p_\perp$ are shown in Fig. 5. The thresholds are similar for the forward and central detectors, but the forward turn-on is sharper, because the multiple scattering error is smaller.

C. TRIGGER RATES

The muon trigger rates are dominated by background sources composed of $\pi \to \mu$ and $K \to \mu$ decay in flight, muons from cosmic rays which penetrate the detector, and hadronic punch through. All three components contribute to the central muon trigger, while only the first one is important for the forward toroids.

To calculate decay in flight a mimimum bias cross section for $\bar{p}$-p collisions at 2 TeV was adopted of the form[2]

$$Ed^3\sigma/dp^3 = (0.47 \times 10^{-24})/(1 + p_\perp)^8 \ \mathrm{cm}^2/\mathrm{GeV}.$$

The results of folding the efficiencies into the pion decay in flight rates are shown in Fig. 6. The central and forward yields are comparable. Kaons contribute an equal amount, while in the central region hadronic punch through adds about another 30%.

The cosmic ray muon rate for the central detector assuming no shielding is 10^4/sec. The trigger requirement reduces this rate to 30 hz. Putting all of these effects together gives the rates of Table 2.

The total trigger rate at a luminosity $L = 10^{30}\ cm^{-2}\ sec^{-1}$ is about 100 hz.

As a stand-alone trigger for the detector this rate is too high, although it might be tolerable when mixed with some other requirement, like a large hadronic E_T cluster, or when two muons or a muon and an electron are required in the same event. In this connection it is interesting to note that a cosmic ray muon which satisfies the single muon trigger is very likely to satisfy the two muon trigger as well. The $p_\perp$ threshold must be raised to decrease the trigger rate. In the central detector this will be done by using roads from the central tracking chamber together with the hit pattern in the muon drift tubes to eliminate lower $p_\perp$ tracks which have scattered or punched through. This road information also greatly decreases the cosmic ray background by sharpening the time window from 1 μ sec to 40 nsec. In the toroids the trigger cell sizes could be decreased to raise the $p_\perp$ threshold at the expense of efficiency at high $p_\perp$. The information from the drift distances themselves could be used to define a rough sagitta and thus tighten the $p_\perp$ threshold. These steps should decrease the trigger rate to a few hz.

The decay $K \to \mu\nu_\mu$ in flight in the central drift chamber can fake a high momentum prompt muon if the decay muon is produced in the bend plane and in the direction opposite to the bend. The transverse momentum of the decay then tends to compensate for the low momentum curvature, creating the appearance of a higher momentum track. This "seagull" effect is a special form of background which must be eliminated by careful measurement of all of the points on the track.

D. MUON DETECTOR UPGRADE

Improvement of the muon system has been proposed as part of the upgrade of the CDF detector. A pair of "super toroids" could be added to the small angle system to increase the angle coverage to 30°, as shown in Fig. 1. These toroids would be instrumented in the same way as the others. In the central region 60 cm thick Fe walls could be added to the sides of the detector, and extra chambers placed around the outside and on top and bottom of the magnet yoke.[3] See Fig. 7. Magnetizing the Fe walls would afford a second rough measurement of muon momentun, thus alleviating the K → μ "seagull" background in the central tracking chamber referred to in Sec. C. These improvements would leave a crack between 30° and 50° on both sides of the collision point which must still be instrumented.

ACKNOWLEDGMENTS

The author is grateful to his many CDF colleagues for stimulating discussions on problems of muon detection. Special thanks go to D. Cline and L. Holloway in this regard. The author also wishes to thank Prof. K. Kondo, Prof. S. Miyashita, Prof. K. Takikawa, and the rest of the Tsukuba and KEK groups for hosting this conference.

REFERENCES

1. CDF Design Report, Fermilab, 1981 (unpublished).
2. UA1 Collaboration, Phys Lett 118B, 167 (1982).
3. S. Cihangir, "A Proposal to Upgrade the CDF Central Muon Detection System" CDF-294, Fermilab, 1985 (unpublished).

Table 1

Geometrical Parameters of the CDF Muon System

	Central	Forward + Backward
$\Delta\phi$	2π	2π
$\Delta\eta$	1.3	3.6
$\Delta\theta$	$55^o < \theta < 125^o$	$3^o < \theta < 17^o$
λ_{DECAY}	1.8 m	6 m
X_{RAD}	17 X_{RAD}Pb	100 X_{RAD} Fe (toroids)
	+ 54 X_{RAD}Fe	+ 50 X_{RAD} Fe (calorimeters)

Table 2

Trigger Rates at 10^{30} cm^{-2} sec^{-1} Luminosity

Toroids (both ends)	60 hz
Central detector	40 hz
Total	100 hz

FIGURE CAPTIONS

1. Elevation view of one side of the detector, showing the small angle toroid system (T), the central and toroid drift chambers (DC), hadronic (H) and electromagnetic (EM) calorimeters, and the central solenoid return yoke (Y). The central magnetic field is 1.5 T, parallel to the colliding beam axis. The toroidal field is 1.8 T, roughly constant in radius, oriented so that the bend plane is the plane formed by the colliding beams and the produced muon. The location of the proposed "super toroids" (S) is also known.
2. End view of an instrumented toroid, showing trigger scintillation counters (S) and drift chamber planes in 15^{o} sectors. The drift chamber cells increase in width as the radius increases. Azimuthal resolution of 5^{o} is achieved with cathode pads.
3. End view of the solenoid field, two wedge modules, and the drift tube array of the central muon system. The calorimeter is 71 X_{RAD} thick and is in a field free region. The impact parameter b at the production vertex is inferred from the slope of the muon track measured by the four drift chambers. An expanded view of the drift chambers is shown below. Alternate sense wires are displaced by 2 mm for ambiguity resolution. The muon coordinate along the wire is measured by charge division.
4. Toroid bend plane showing the tower geometry of the drift chamber cells and the basic 1 * 3 * 3 trigger pattern. Measurement of the muon orbit is done from the drift times in the three cells, and is dominated by multiple scattering error for muons below about 200 GeV/c. The cell size is exaggerated in the Figure for clarity.
5. Trigger efficiencies as a function of $p_{\perp}$ for the toroid (T) and central (C) detectors, using the triggers defined in the text.
6. Differential rates for $\pi^{+} + \pi^{-}$ production (top curve), and for muons from pion decay in flight for the central muon detector

and the forward detector at 10^{o}. The total event rate at a luminosity $L = 10^{30}\ cm^{-2}\ sec^{-1}$ is 50 khz.

7. Extra Fe walls added to the sides of the central detector to decrease the hadronic punch through and improve the muon trigger in the central region. More chambers would also be added above and below the detector to exploit the Fe return yoke of the solenoid magnet, and the gap shown in the Fe yoke would be filled with non-ferromagnetic absorber.

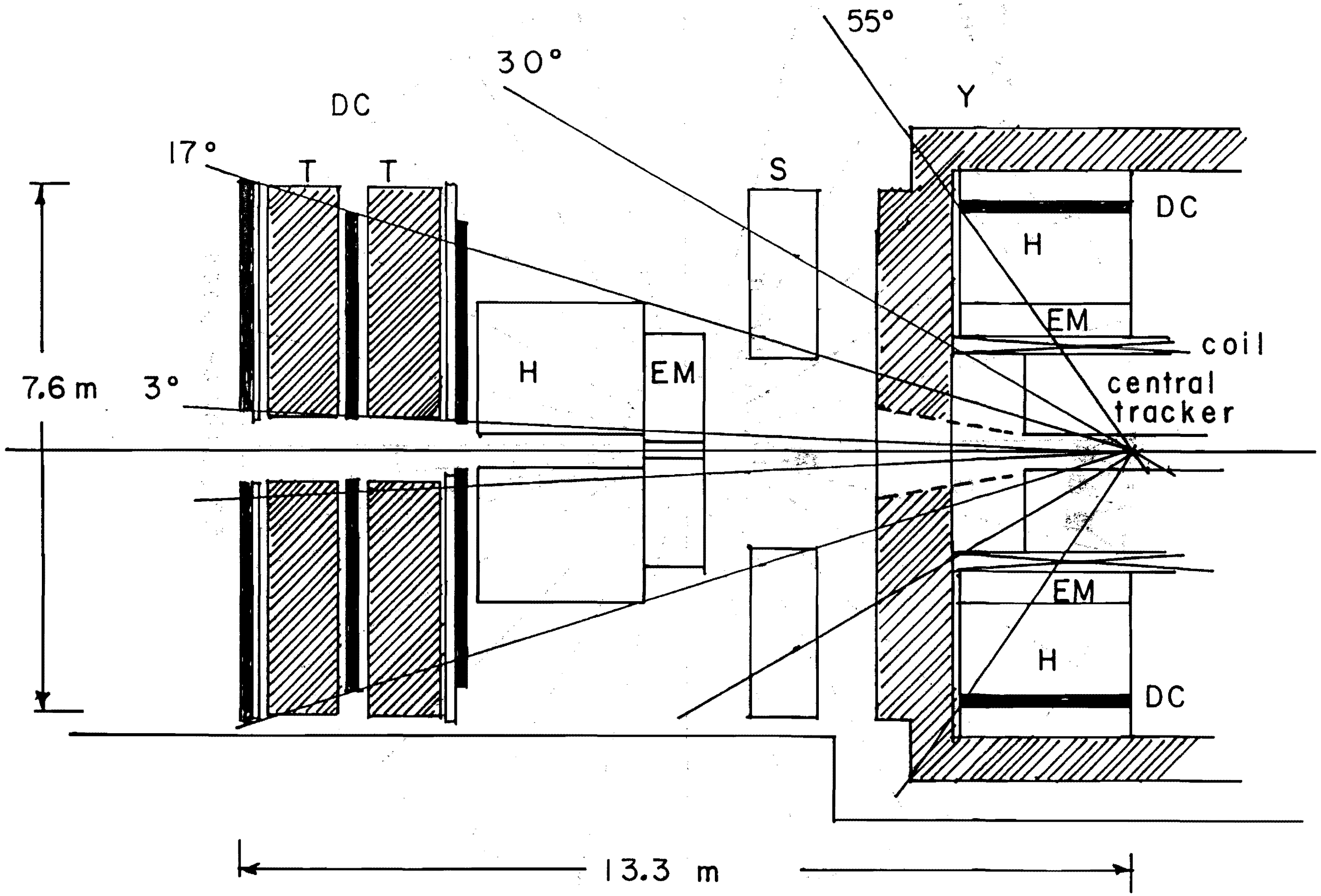
55°
30°
DC
Y
17°
T
T
S
DC
H
EM
coil
central
tracker
7.6 m
3°
H
EM
EM
H
DC
13.3 m

Fig. 1

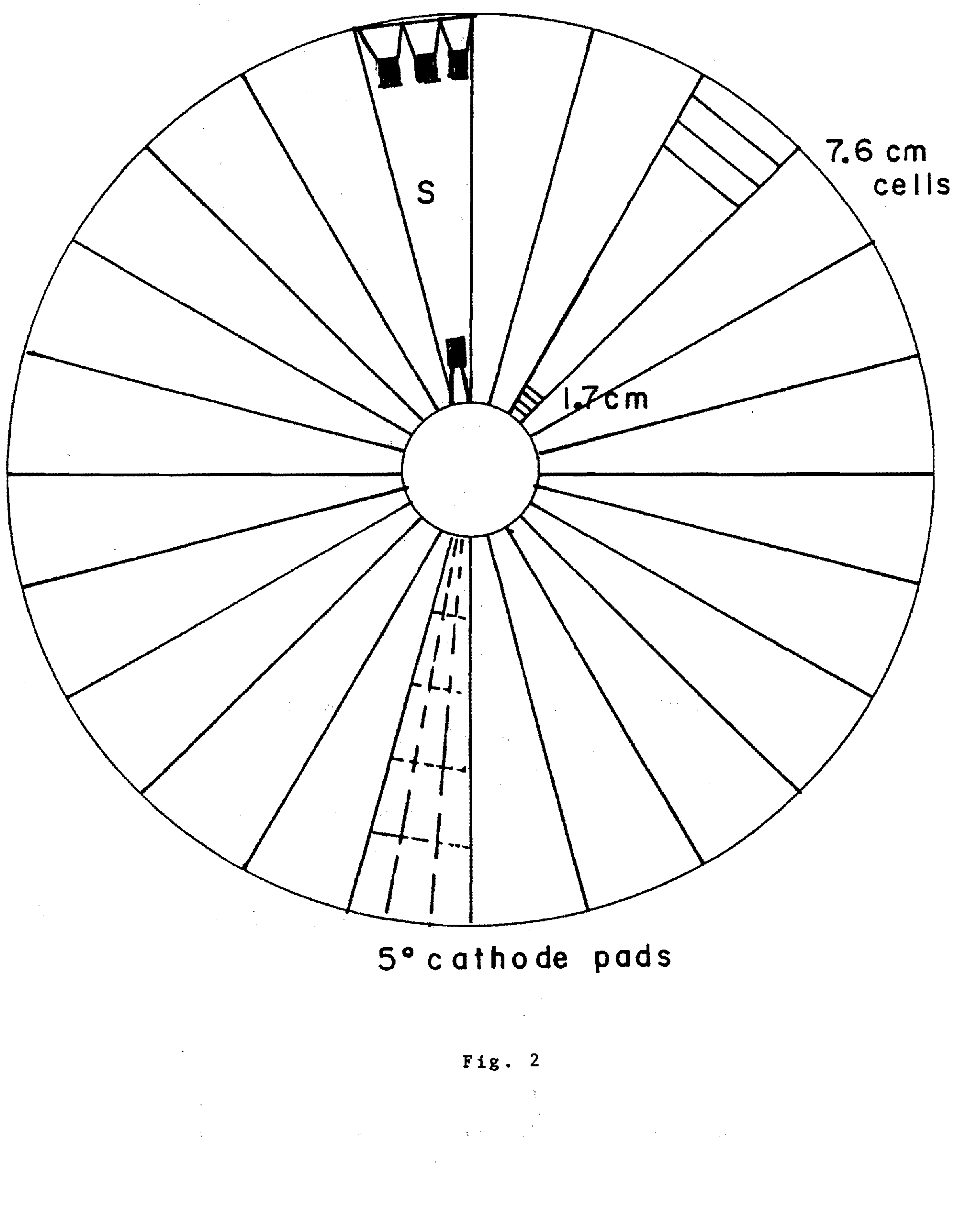

Fig. 2

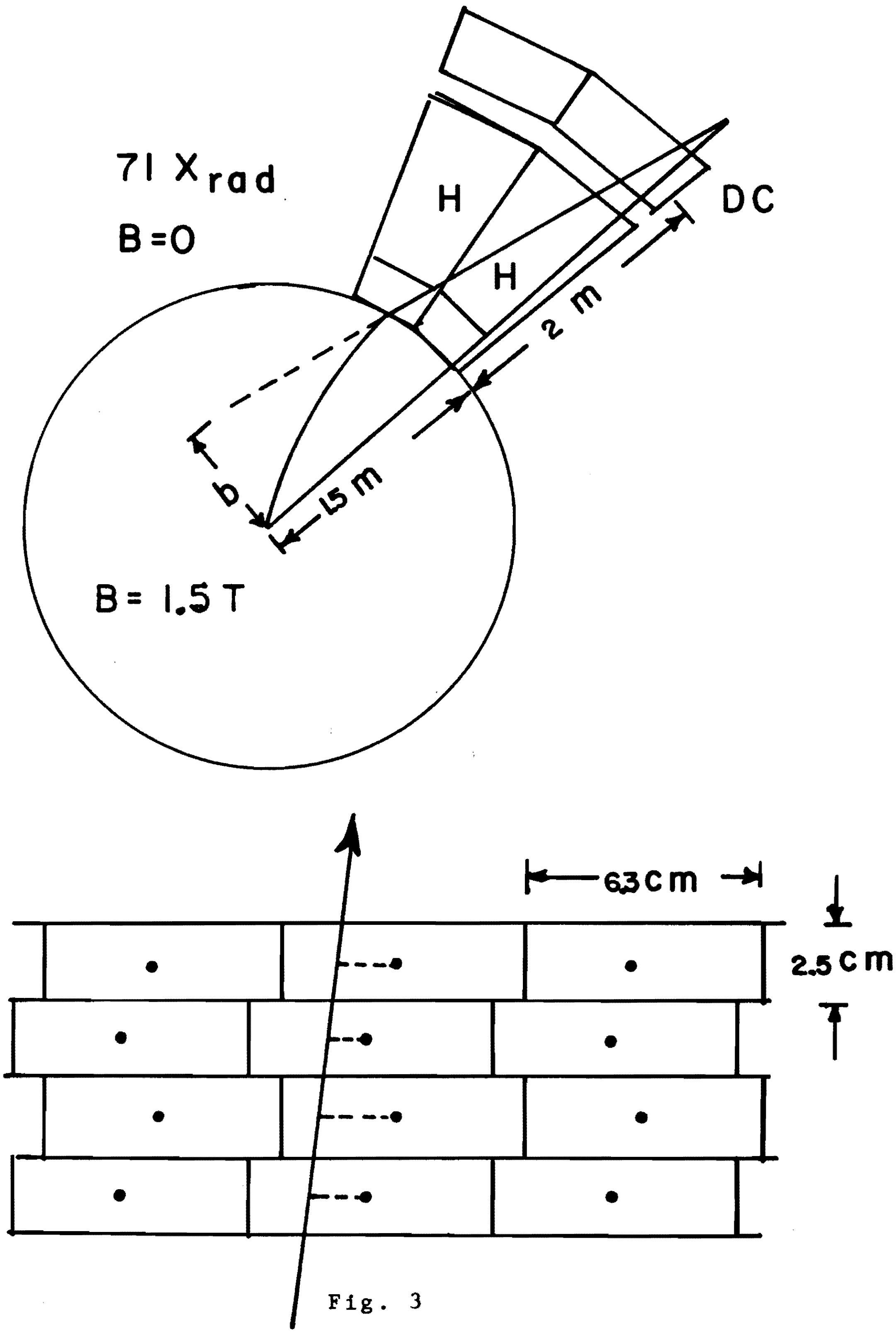

Fig. 3

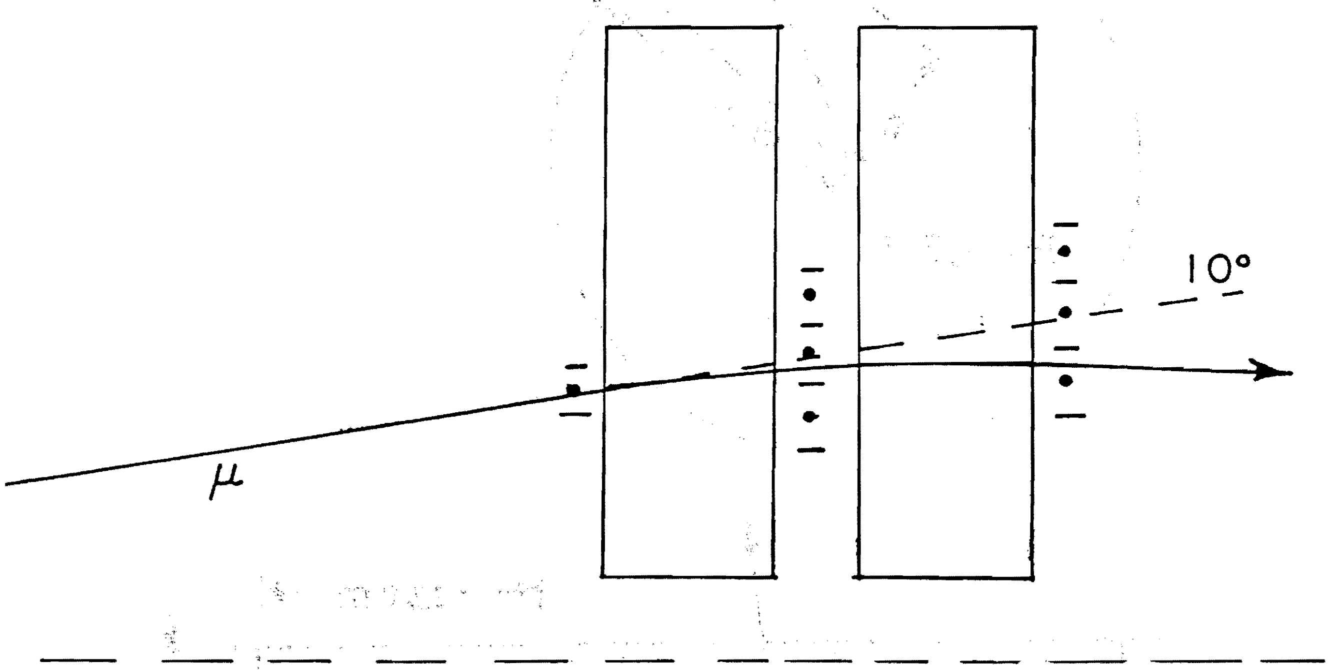

Fig. 4

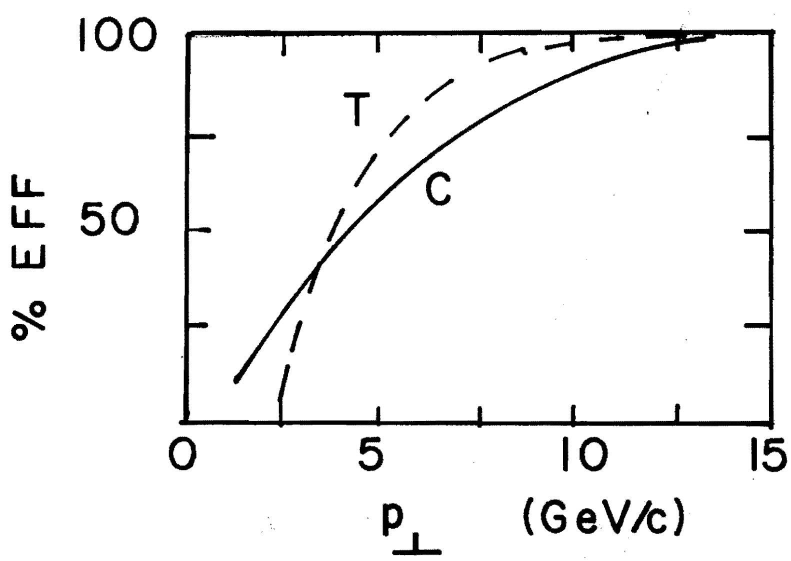

Fig. 5

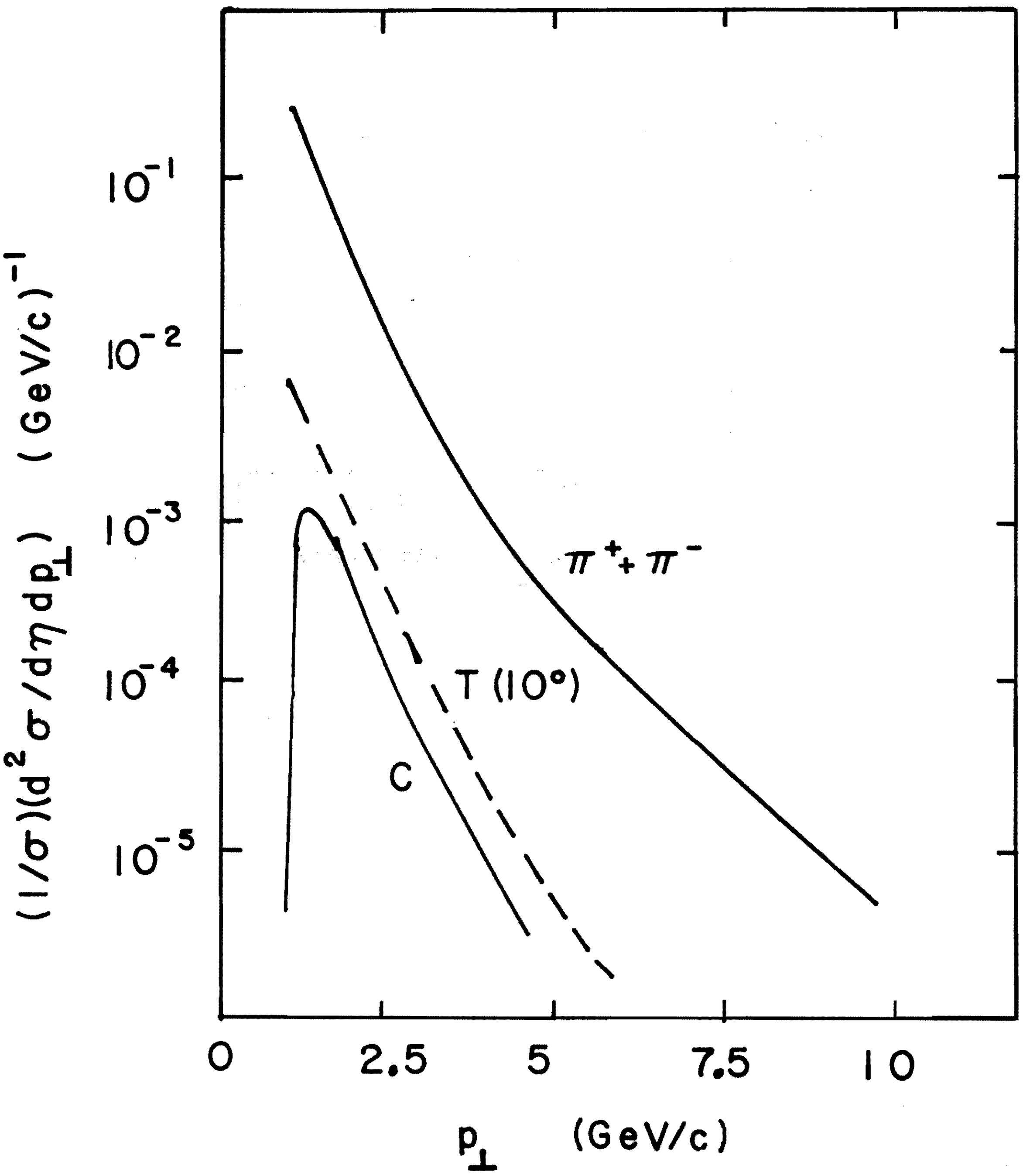
10^{-1}
10^{-2}
10^{-3}
10^{-4}
10^{-5}
$(1/\sigma)(d^2\sigma/d\eta\, dp_\perp)$ $(\mathrm{GeV/c})^{-1}$
$\pi^+ + \pi^-$
T (10°)
C
0
2.5
5
7.5
10
$p_\perp$ (GeV/c)

Fig. 6

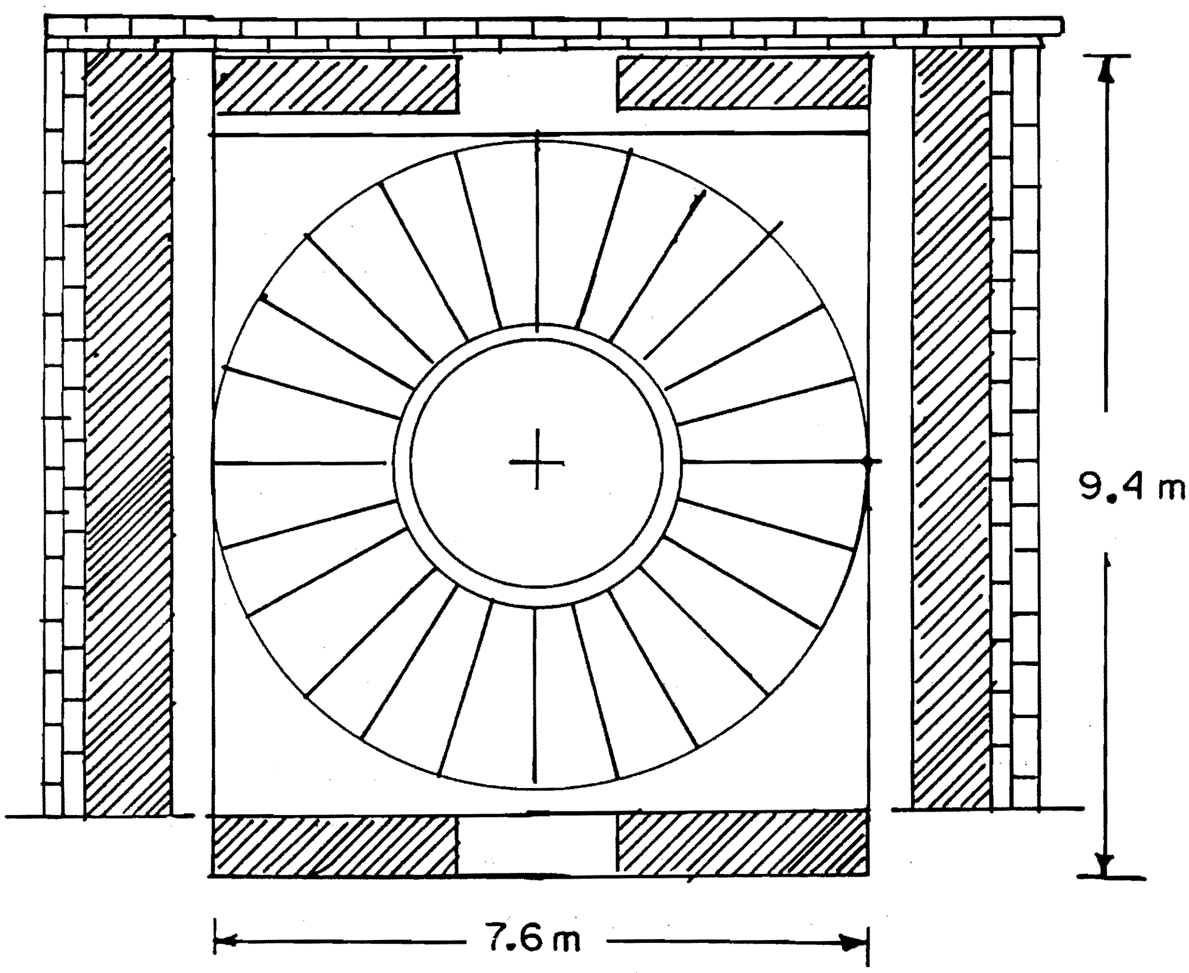

Fig. 7